Young inner core inferred from Ediacaran ultra-low geomagnetic field intensity

Richard K. Bono [1,4], John A. Tarduno [1,2]*, Francis Nimmo [3] and Rory D. Cottrell [1]

An enduring mystery about Earth has been the age of its solid inner core. Plausible yet contrasting core thermal conductivity values lead to inner core growth initiation ages that span 2 billion years, from ~0.5 to >2.5 billion years ago. Palaeomagnetic data provide a direct probe of past core conditions, but heretofore field strength data were lacking for the youngest predicted inner core onset ages. Here we present palaeointensity data from the Ediacaran (~565 million years old) Sept-Îles intrusive suite measured on single plagioclase and clinopyroxene crystals that hosted single-domain magnetic inclusions. These data indicate a time-averaged dipole moment of ~0.7×10^{22} A m², the lowest value yet reported for the geodynamo from extant rocks and more than ten times smaller than the strength of the present-day field. Palaeomagnetic directional studies of these crystals define two polarities with an unusually high angular dispersion ($S = ~26°$) at a low latitude. Together with 14 other directional data sets that suggest a hyper-reversal frequency, these extraordinary low field strengths suggest an anomalous field behaviour, consistent with predictions of geodynamo simulations, high thermal conductivities and an Ediacaran onset age of inner core growth.

To establish the age of the inner core depends on how fast heat is removed from the core; the difference between this heat flux and the adiabatic value controls whether a dynamo can operate. Thus, uncertainty in the value of core thermal conductivity[1,2] led to wide variations in the estimates of inner core age. Evidence for a geomagnetic field from extant rocks extends to as old as 3.45 billion years ago (Ga) (ref. [3]), whereas palaeomagnetic data from zircons suggest a geodynamo as old as 4.2 Ga (ref. [4]) (Supplementary Section 1.0). Recent models of the chemical precipitation of MgO (ref. [5,6]) and SiO_2 (ref. [7]) provide alternatives for powering the most ancient geodynamo, but they leave the age of the inner core unanswered. Anomalous geomagnetic activity might be expected when the convective regime of the core changed, and latent heat release associated with the freezing of iron at the nascent inner core boundary became an important energy source for driving the geodynamo. This has been predicted by some numerical dynamo simulations[8], but heretofore it has not been seen in the history of geomagnetic field strength (palaeointensity).

A rigorous recent review of the palaeointensity record noted a potential rise in values in Mesoproterozoic times (~1.2 Ga), which was suggested to be a sign of inner core growth[9]. However, the data used to define the palaeointensity increase included very low unblocking temperature magnetizations known to be contaminated by viscous remanent magnetizations which, if unrecognized, can lead to palaeofield overestimates. When biased data are removed, the meaning of the remaining rise is as yet uncertain because it is no greater than that seen in analyses of similar rocks formed during the past 15 million years[10], a time when inner core growth clearly did not start.

The highest core conductivity values predict ages of the inner core growth near 500–600 million years ago (Ma) (refs [11–13]), but there is a paucity of palaeointensity values of this age, and no values that record the time-averaged geomagnetic field. The ~565 Ma Sept-Îles intrusive suite (SIIS)[14], a predominantly mafic layered intrusion

(Supplementary Fig. 1), provides the opportunity to fill this critical palaeointensity gap. We applied the single-crystal palaeointensity (SCP) method[15,16] (Methods), which relies on the study of individual silicate crystals that contain magnetic inclusions. These inclusions can have favourable magnetic recording properties[15–17], whereas the silicate host can protect the inclusions from alteration. Rock magnetic analyses of plagioclase feldspars from anorthosites of the SIIS show a non-interacting single-domain behaviour[14] and thus meet robust palaeointensity recording criteria[18]. Electron microscopy and microprobe analyses indicate that the magnetization is held by needle-shaped inclusions in the feldspars[14].

We first sought an approximate palaeointensity value by total thermal remanent magnetization (TTRM) experiments. A plagioclase crystal was first thermally demagnetized using a CO_2 laser[19] (Methods), which removed its natural remanent magnetization (NRM). Next, a TTRM was applied at the maximum observed unblocking temperature (520 °C) in a 60 μT field. The palaeofield value was obtained by comparing the TTRM and NRM intensities. Measurements were conducted using a three-component 2G DC SQUID magnetometer with high-resolution sensing coils in the magnetically shielded laboratory at the University of Rochester (ambient field <200 nT). These analyses suggest an unusually weak mean palaeointensity of 8.7 ± 4.5 μT (Supplementary Table 1).

We next proceeded to a more thorough investigation using Thellier–Coe palaeointensity analyses that incorporates partial thermal remanent magnetization (PTRM) checks to assess alteration (Fig. 1, Methods and Supplementary Fig. 2). We attempted 101 experiments and subsequently assessed them using the following criteria: Category A, at least four steps must be included in the NRM versus thermoremanent magnetization (TRM) slope, the R^2 of the NRM/TRM slope fit must be greater than 0.9, the field-off NRM values must trend to the origin of the orthogonal vector plots with a maximum angular dispersion ≤10° and the PTRM checks must be within 10%. We also considered two

[1]Department of Earth & Environmental Sciences, University of Rochester, Rochester, NY, USA. [2]Department of Physics & Astronomy, University of Rochester, Rochester, NY, USA. [3]Department of Earth and Planetary Sciences, University of California, Santa Cruz, CA, USA. [4]Present address: Geomagnetism Laboratory, University of Liverpool, Liverpool, UK. *e-mail: john.tarduno@rochester.edu
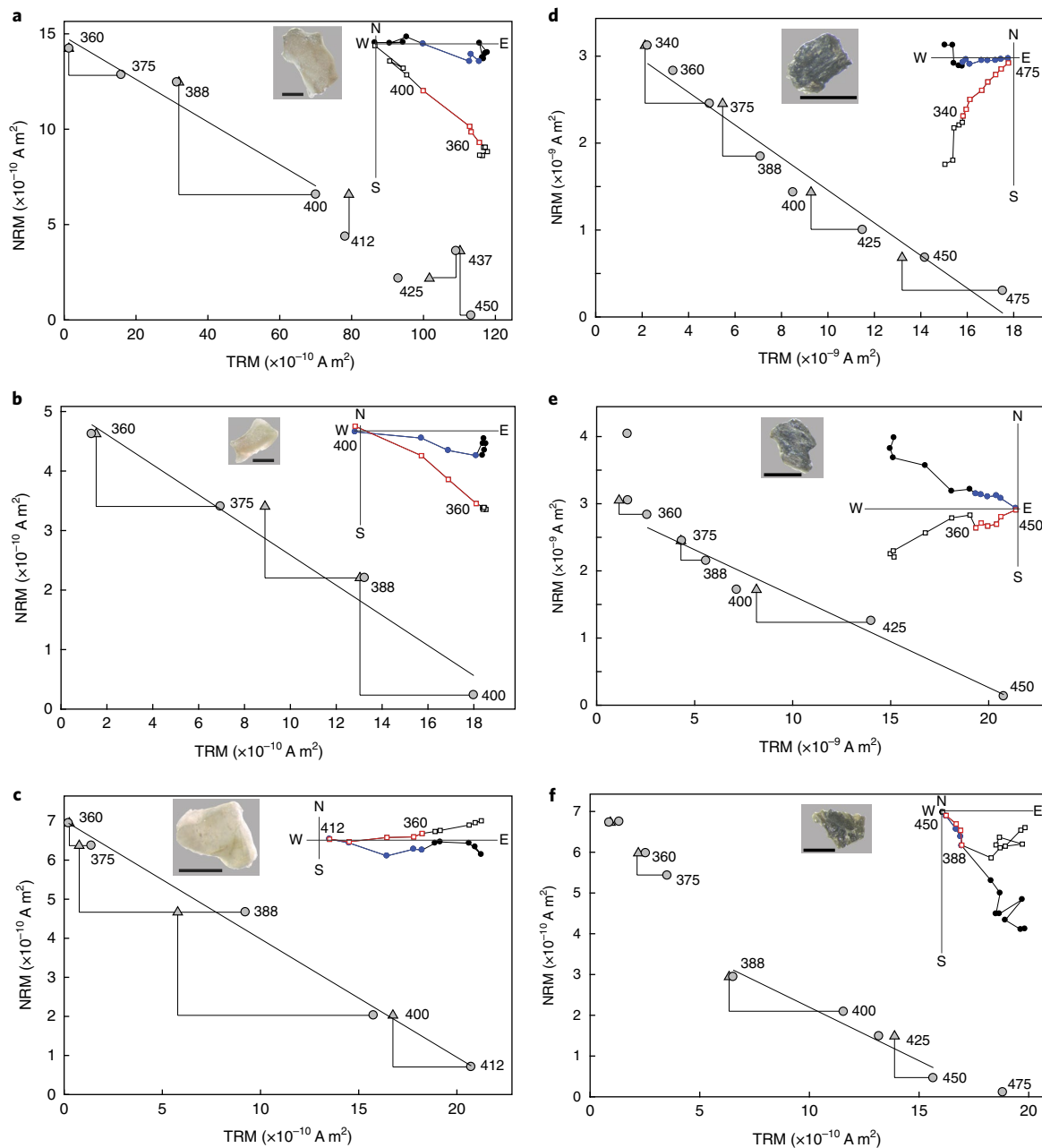
Fig. 1 | Thellier–Coe palaeointensity experiments of single silicate crystals from Sept-Îles anorthosite. The inset photographs show the measured crystals (Methods). Scale bars, 1 mm. The upper right insets are the orthogonal vector plots of the field-off magnetizations (squares, inclination; circles, declination; red and blue lines denote temperature fits included in the line fit). **a–d**, NRM versus TRM (circles) and PTRM checks (triangles). The labelled steps show the temperature (°C). Palaeointensity value shown in the lower left corner. **a**, Feldspar si1-2d10 (crystal removed completely from slide), palaeointensity 3.44 μT. **b**, Feldspar si1-2d09, palaeointensity 7.71 μT. **c**, Feldspar si1-2b20 (crystal removed completely from slide), palaeointensity 9.13 μT. **d**, Clinopyroxene si1-3cpx23, palaeointensity 2.87 μT. **e**, Clinopyroxene si1-3cpx19, palaeointensity 2.09 μT. **f**, Clinopyroxene si1-3cpx15, palaeointensity 4.06 μT.

Category B experiments in which only one criterion was relaxed (Supplementary Table 2). Applied fields of 30 μT and 60 μT were used. For remanences isolated between 360 and 412 °C, these yielded a mean palaeointensity of 6.6 ± 3.7 μT ($n = 7$), which supports the low field indicated by the initial TTRM estimate. Note that the field estimates based on different applied fields (30 μT, 7.0 ± 3.9 μT; 60 μT, 5.6 ± 4.4 μT) are indistinguishable, and therefore there is no evidence for a significant non-linearity in the relationship between the strength of the applied TRM and the recovered NRM palaeointensity[20]. The success rate of the Thellier–Coe experiments is approximately 12%. The primary reason for the rejection of data is the apparent alteration at temperatures less than 400 °C (60% of the values), which we infer to indicate the presence of minor sulfides (Supplementary Fig. 3) that were missed irrespective of the attempts to screen samples using microscopic analyses. Data were also rejected because of failed PTRM checks at temperatures >400 °C (21%) and principal component fits that did not trend towards the origin of the orthogonal vector plots (6%). However, we also note that some of the apparent experimental failures may be related to noise due to the difficulty of measuring the weak NRMs carried by the feldspar crystals (initial NRM $\sim 1 \times 10^{-10}$ A m²).

As an additional examination of the remanence, we conducted SCP analyses on SIIS anorthosite clinopyroxene. Electron microscopy revealed titanomagnetite needle inclusions with a characteristic single-domain behaviour[15,21] (Supplementary Fig. 4). These crystals have NRM intensities 1–3 orders of magnitude greater than those of SIIS feldspars. An initial TTRM measurement again yielded a low field value of 7.3 µT. Thellier–Coe analyses(25) were conducted using applied fields of 15 µT and 30 µT. The data obtained at temperatures between 360 and 450 °C are suitable for a palaeointensity determination (Fig. 1 and Supplementary Fig. 2). These temperatures are compatible with the high levels of titanomagnetite observed in inclusions (Supplementary Fig. 4) and Curie temperatures well below typical exsolution temperatures. Kinetics are sluggish at these temperatures, and those at which the SIIS plagioclase magnetization has been isolated support a high-temperature origin of the inclusions and the conclusion that the magnetization is thermoremanent[21] (Supplementary Section 1.1). The Thellier–Coe analyses on SIIS clinopyroxene, evaluated using the same criteria as for the SIIS feldspars (Methods), yield a mean palaeointensity of $3.6 \pm 1.8\,\mu T$ ($n = 8$), which supports the low field indicated by the initial TTRM estimate. The field estimates based on different applied fields (15 µT, $3.1 \pm 1.3\,\mu T$; 30 µT, $3.9 \pm 2.0\,\mu T$) are again indistinguishable. The success rate of the Thellier-Coe experiments is approximately 32%. Some data were rejected due to poor PTRM checks (12% of total number of samples run). Data were also rejected because of the failure of the sample to acquire the applied lab field (28%) and field-off directions that were unstable or did not trend to the origin of orthogonal vector plots (28%). The clinopyroxene mean is lower (but within uncertainty) of the feldspar mean intensity. As the clinopyroxene data are isolated at a slightly higher temperature than those of the feldspar, this may record a difference in the field during cooling. However, because we are interested in average field values, we continue below by pooling the data.

The time-averaged field

We next address this key question of time averaging. The geomagnetic field at a radius r, colatitude θ, longitude ϕ and time t can be described by the gradient of the scalar potential (Φ):

$$\Phi(r,\theta,\phi,t) = r_E \sum_{l=1}^{\infty} \sum_{m=0}^{l} \left(\frac{r_E}{r}\right)^{l+1} P_l^m(\cos\theta) \left[g_l^m(t)\cos m\phi + h_l^m(t)\sin m\phi\right] \quad (1)$$

where P_l^m are partially normalized Schmidt functions, r_E is the radius of Earth and the Gauss coefficients g_l^m and h_l^m describe the size of spatially varying fields. The spatial and temporal variability with time indicates that instantaneous field records, such as those recorded by a rapidly cooled lava or dike, could depart widely from a value dominated by the lower-order terms (that is, g_1^0). Instead, to make conclusions on the geodynamo we require time-averaged values, also known as palaeomagnetic dipole moments[15], that average this variability; the relatively slow cooling of the SIIS suggests the palaeointensity data can satisfy this criterion (Supplementary Section 1.1).

The efficiency with which remanence is acquired is dependent, in part, on the rate at which the sample cooled. We consider a cooling of ~75 kyr (ref. [14]) for the unblocking temperatures at which the characteristic remanence is defined, which leads to a cooling rate correction factor of ~1.5 (Supplementary Section 1.1). This suggests that the true palaeofield strength recorded by the SIIS feldspar and clinopyroxene is 33% weaker than the uncorrected Thellier–Coe palaeointensity measurements indicate, which results in palaeointensity estimates of $3.4 \pm 2.1\,\mu T$ ($n = 15$). Although the needle-like shapes of the magnetic inclusions in the feldspars and clinopyroxenes support single-domain characteristics, they also introduce the potential for remanence anisotropy. As a final check on the recording fidelity of the Thellier–Coe palaeointensity experiments, a six-heating anisotropy protocol was performed (Methods). In five experiments that met the selection criteria, we calculated a correction factor (Methods), which ranges from 0.7 to 1.2, leading to palaeointensity estimates of $3.0 \pm 1.2\,\mu T$ (including the cooling rate correction, Supplementary Table 2). Using a palaeolatitude of 18.4° calculated from palaeomagnetic analyses of oriented SIIS feldspars[14], the mean palaeointensity measured from all the Thellier–Coe SCP experiments corrected for cooling rate suggests a palaeomagnetic dipole moment of $0.76 \pm 0.47 \times 10^{22}\,A\,m^2$ and $0.67 \pm 0.27 \times 10^{22}\,A\,m^2$ for our preferred estimate that incorporates anisotropy and values corrected for the cooling rate.

Weak field state and inner core

Near antipodal magnetic directions observed at subcentimetre length scales in the SIIS feldspars suggest a very high reversal rate[14] accompanied the ultra-low intensity at ~565 Ma. This behaviour is reminiscent of that of the Late Jurassic (~165 Ma), when the geomagnetic field underwent >10 reversals per million years[22], but the field at ca. 565 Ma, defined by SCP analyses, is ~5 times lower in strength than that of the Jurassic. Some low field intensities, among values higher than the present-day field, were reported for the Devonian[23], but these, if of primary origin, do not record the time-averaged field and the nominal mean is 3–4 times higher than the SIIS SCP value. The ultra-low intensity at ~565 Ma is greater than the external fields that would be induced by the solar wind impinging on the atmosphere in the absence of a core dynamo[24]. Thus, the geodynamo existed but was in an extraordinary state (Fig. 2). Emerging data sets of instantaneous records of Ediacaran field strengths support this interpretation[25].

With the caveats that only a few time-averaged values are available and bulk rocks contain non-ideal magnetic carriers[18], a trend to a lower field strength from Archaean to Ediacaran times, with superimposed variability, is hinted at by a new database of reliable Precambrian palaeointensity values (Supplementary Section 1.2 and Supplementary Tables 3–6). Directional data from the study of 12 volcanic/intrusive units[26] and three sedimentary sequences[27] formed between 533 and 615 Ma suggest a hyper-reversal rate and/or unusual field behaviour (Fig. 2 and Supplementary Table 7). A consideration of the angular dispersion of single silicate directions from the Sept-Îles indicates very high values ($S = \sim 26°$) at a low latitude, which exceed the times of rapid reversals in the Phanerozoic (Supplementary Section 1.3 and Supplementary Fig. 5).

These observations have similarities with several aspects of numerical geodynamo simulations. The long-term dipole decay prior to inner core nucleation is similar to that predicted using magnetic scaling and thermal evolution models[28], but the intensity change predicted by these models is much smaller than the observations. The ultra-low intensity and hyper-reversal/unusual field behaviour inferred evoke the weak field dynamo state when the ratio of magnetic to kinetic energy (ME/KE) is of order unity. Both Driscoll[8] and Landeau et al.[29], employing different approaches to thermal evolution, predict a weak field state during the onset of inner core growth. The core and mantle thermal evolution model of Driscoll[8] predicts a weak field state prior to inner core nucleation, qualitatively similar to the period of Ediacaran field instability suggested by the available observations, but ~4 times longer in duration. Landeau et al.[29] prescribe a core–mantle boundary heat flux history and predict a weak field state at, and before, inner core nucleation, but it is transient, lasting on the order of a magnetic diffusion time. The new view of Precambrian field evolution (Fig. 2) can serve as a template for further refinements of these models, which includes those that consider chemical precipitation to drive the geodynamo. Overall, the available model predictions, our new data from the ~565 Ma Sept-Îles rocks, and other global
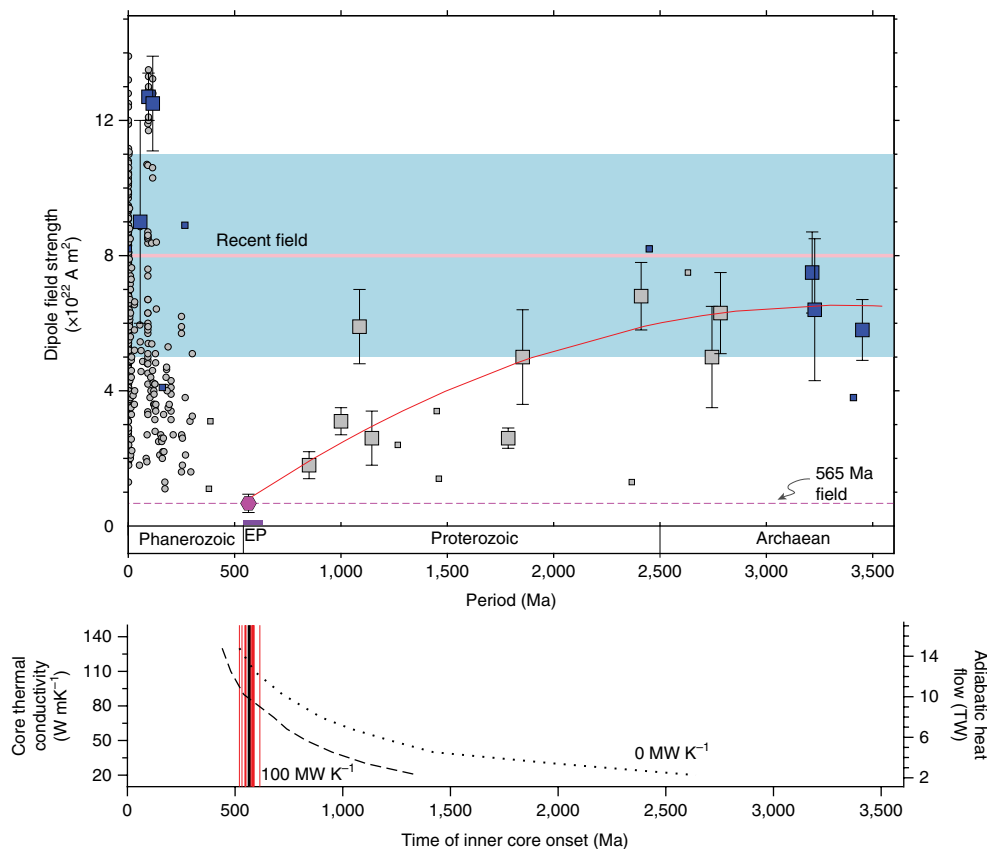
Fig. 2 | Geomagnetic field strength and inner core growth. Estimates (upper panel) from SCP studies (blue squares) and bulk rock studies (grey squares) shown from a new database that emphasizes time averaging (Supplementary Tables 4–6). Large squares, time-averaged palaeomagnetic dipole moments; small squares, virtual dipole moments; grey circles, select Phanerozoic virtual dipole moments (Supplementary Section 1.2); magenta hexagon, time-averaged SCP result (this study) with 1σ uncertainty; blue field, modern geomagnetic field; red line, weighted second-order polynomial regression of Precambrian field strength data. The select Precambrian palaeointensity data show a trend of decreasing strength with time which can be modelled with a linear fit or polynomial fit (Supplementary Section 1.2). EP, Ediacaran period. Modelled inner core onset time as a function of core thermal conductivity (bottom panel) for vigorous (dashed line) and weak (dotted line) dynamos[13] assuming a constant core–mantle boundary heat flow sufficient to generate the specified rate of entropy production prior to the inner core onset (Supplementary Section 1.4). The right-hand axis shows the core–mantle boundary heat flow required in the 0 MW K⁻¹ entropy production case, that is the adiabatic value. Red lines, reported intervals of an unstable geomagnetic field (Supplementary Table 7); solid vertical line, age of the Sept-Îles intrusion.

observations suggest the geodynamo approached collapse (ME/KE < 1) in the late Precambrian as inner core growth commenced. Assuming that the dynamo required an entropy production rate of 0–100 MW K⁻¹ prior to inner core nucleation, a nucleation age of 565 Ma implies relatively high thermal conductivities in the range of 86–118 W mK⁻¹ (Fig. 2 and Supplementary Section 1.4).

The Ediacaran age of the ultra-low geomagnetic field intensity is intriguing. Suggestions that a decreased magnetic shielding had an effect on the profound changes in animal evolution that marked this, and the succeeding early Cambrian interval, are controversial[30,31]. Nevertheless, the field intensity was, indeed, extraordinarily low and the long-term magnetopause stand-off distance would have been <4.5 Earth radii, a value less than that of recent severe solar storms in which coronal mass ejections compress the magnetosphere on hour timescales[3,24]. Although the ultra-low field intensity at ~565 Ma is unprecedented, it may mark the start of a geodynamo with ~200 Myr cycles in behaviour linked to mantle convection[16,22]. A young inner core also indicates a high heat flux (~15 TW) into the mantle (Supplementary Section 1.4), and thus reduces the overall mantle cooling rate. This may help to explain the discrepancy between estimates of mantle cooling rates from petrology in the latter half of Earth's history[32] and from the mantle heat production rate relative to the Earth's surface heat flow (that is, the Urey ratio[11,33]).

Online content

Any methods, additional references, Nature Research reporting summaries, source data, statements of data availability and associated accession codes are available at https://doi.org/10.1038/s41561-018-0288-0.

References

1. Ohta, K., Kuwayama, Y., Hirose, K., Shimizu, K. & Ohishi, Y. Experimental determination of the electrical resistivity of iron at Earth's core conditions. *Nature* **534**, 95–98 (2016).
2. Konôpková, Z., McWilliams, R. S., Gómez-Pérez, N. & Goncharov, A. F. Direct measurement of thermal conductivity in solid iron at planetary core conditions. *Nature* **534**, 99–101 (2016).
3. Tarduno, J. A. et al. Geodynamo, solar wind, and magnetopause 3.4 to 3.45 billion years ago. *Science* **327**, 1238–1240 (2010).
4. Tarduno, J. A., Cottrell, R. D., Davis, W. J., Nimmo, F. & Bono, R. K. A Hadean to Paleoarchean geodynamo recorded by single zircon crystals. *Science* **349**, 521–524 (2015).
5. O'Rourke, J. G. & Stevenson, D. J. Powering Earth's dynamo with magnesium precipitation from the core. *Nature* **529**, 387–389 (2016).
6. Badro, J., Siebert, J. & Nimmo, F. An early geodynamo driven by exsolution of mantle components from Earth's core. *Nature* **536**, 326–328 (2016).

7. Hirose, K. et al. Crystallization of silicon dioxide and compositional evolution of the Earth's core. *Nature* **543**, 99–102 (2017).
8. Driscoll, P. Simulating 2 Ga of geodynamo history. *Geophys. Res. Lett.* **43**, 5680–5687 (2016).
9. Biggin, A. J. et al. Palaeomagnetic field intensity variations suggest Mesoproterozoic inner-core nucleation. *Nature* **526**, 245–248 (2015).
10. Smirnov, A. V., Tarduno, J. A., Kulakov, E. V., McEnroe, S. A. & Bono, R. K. Palaeointensity, core thermal conductivity and the unknown age of the inner core. *Geophys. J. Int.* **205**, 11901195 (2016).
11. Driscoll, P. & Bercovici, D. On the thermal and magnetic histories of Earth and Venus: influences of melting, radioactivity, and conductivity. *Phys. Earth Planet. Inter.* **236**, 36–51 (2014).
12. Labrosse, S. Thermal evolution of the core with a high thermal conductivity. *Phys. Earth Planet. Inter.* **247**, 36–55 (2015).
13. Nimmo, F. in *Treatise on Geophysics* 2nd edn (ed. Schubert, G.) 201–219 (Elsevier, Amsterdam, 2015).
14. Bono, R. K. & Tarduno, J. A. A stable Ediacaran Earth recorded by single silicate crystals of the ca. 565 Ma Sept-Îles intrusion. *Geology* **43**, 131–134 (2015).
15. Tarduno, J. A., Cottrell, R. D. & Smirnov, A. V. The paleomagnetism of single silicate crystals: recording the geomagnetic field during mixed polarity intervals. *Rev. Geophys.* **44**, RG1002 (2006).
16. Tarduno, J. A. Geodynamo history preserved in single silicate crystals: origins and long-term mantle control. *Elements* **5**, 217–222 (2009).
17. Dunlop, D. J. & Özdemir, Ö. *Rock Magnetism: Fundamentals and Frontiers* (Cambridge Univ. Press, Cambridge, 1997).
18. Smirnov, A. V., Kulakov, E. V., Foucher, M. S. & Bristol, K. E. Intrinsic paleointensity bias and the long-term history of the geodynamo. *Sci. Adv.* **3**, e1602306 (2017).
19. Tarduno, J. A., Cottrell, R. D., Watkeys, M. K. & Bauch, D. Geomagnetic field strength 3.2 billion years ago recorded by single silicate crystals. *Nature* **446**, 657–660 (2007).
20. Selkin, P. A., Gee, J. S. & Tauxe, L. Nonlinear thermoremanence acquisition and implications for paleo-intensity data. *Earth Planet. Sci. Lett.* **256**, 81–89 (2007).
21. Feinberg, J. M., Scott, G. R., Renne, P. R. & Wenk, H.-R. Exsolved magnetite inclusions in silicates: features determining their remanence behavior. *Geology* **33**, 513–516 (2005).
22. Tarduno, J. A. & Cottrell, R. D. Dipole strength and variation of the time-averaged reversing and nonreversing geodynamo based on Thellier analyses of single plagioclase crystals. *J. Geophys. Res.* **110**, B11101 (2005).
23. Shcherbakova, V. V. et al. Was the Devonian geomagnetic field dipolar or multipolar? Palaeointensity studies of Devonian igneous rocks from the Minusa Basin (Siberia) and the Kola Peninsula dykes, Russia. *Geophys. J. Int.* **209**, 1265–1286 (2017).
24. Tarduno, J. A., Blackman, E. G. & Mamajek, E. E. Detecting the oldest geodynamo and attendant shielding from the solar wind: implications for habitability. *Phys. Earth Planet. Inter.* **233**, 68–87 (2014).
25. Shcherbakova, V., Bakhmutov, V., Shcherbakov, V. & Zhidkov, G. Extremely low palaeointensities in the Neoproterozoic obtained on volcanic rocks from the Ukrainan shield. *Geophys. Res. Abstr.* **20**, EGU2018-11598 (2018).
26. Halls, H. C., Lovette, A., Hamilton, M. & Söderlund, U. A paleomagnetic and U–Pb geochronology study of the western end of the Grenville dyke swarm: rapid changes in paleomagnetic field direction at ca. 585 Ma related to polarity reversals? *Precambrian Res.* **257**, 137–166 (2015).
27. Bazhenov, M. L. et al. Late Ediacaran magnetostratigraphy of Baltica: evidence for magnetic field hyperactivity? *Earth Planet. Sci. Lett.* **435**, 124–135 (2016).
28. Aubert, J., Labrosse, S. & Poitou, C. Modelling the palaeo-evolution of the geodynamo. *Geophys. J. Int.* **179**, 1414–1428 (2009).
29. Landeau, M., Aubert, J. & Olson, P. The signature of inner-core nucleation on the geodynamo. *Earth Planet. Sci. Lett.* **465**, 193–204 (2017).
30. Doglioni, C., Pignatti, J. & Coleman, M. Why did life develop on the surface of the Earth in the Cambrian? *Geosci. Front.* **7**, 865–873 (2016).
31. Meert, J. G., Levashova, N. M., Bazhenov, M. L. & Landing, E. Rapid changes of magnetic field polarity in the late Ediacaran: linking the Cambrian evolutionary radiation and increased UV-B radiation. *Gondwana Res.* **34**, 149–157 (2016).
32. Herzberg, C., Condie, K. & Korenaga, J. Thermal history of the Earth and its petrological expression. *Earth Planet. Sci. Lett.* **292**, 79–88 (2010).
33. O'Rourke, J. G., Korenaga, J. & Stevenson, D. J. Thermal evolution of Earth with magnesium precipitation in the core. *Earth Planet. Sci.* **458**, 263–272 (2017).

Acknowledgements

Author contributions

J.A.T. and R.K.B. conducted the field studies. R.K.B. conducted the palaeomagnetic measurements on the feldspars and R.D.C. measured clinopyroxenes; both data sets were analysed by R.K.B., R.D.C. and J.A.T. Electron microscope analyses were conducted by J.A.T. Core thermal conductivity models were provided by F.N. All the authors participated in the writing of the manuscript. J.A.T. conceived and supervised the study. We thank J. Feinberg for helpful comments.

Competing interests

The authors declare no competing interests.

Additional information

Supplementary information is available for this paper at https://doi.org/10.1038/s41561-018-0288-0.

Reprints and permissions information is available at www.nature.com/reprints.

Correspondence and requests for materials should be addressed to J.A.T.

Publisher's note: Springer Nature remains neutral with regard to jurisdictional claims in published maps and institutional affiliations.

Methods

Sample preparation, heating and measurement. Individual plagioclase feldspar crystals were isolated from ~1 mm thick microscope sections of Sept-Îles anorthosites following the protocol of Bono and Tarduno[14]. Opaque minerals were removed prior to subsampling. Samples selected for the palaeointensity study satisfied the following criteria: free of visible inclusions under ×10 magnification, have a NRM greater than 1×10^{-10} A m^2 and are ~1–4 mm^2 in size. Unoriented samples were mounted on quartz sample holders (sample holder NRMs ~1×10^{-12} A m^2) for palaeointensity experiments. Unoriented individual clinopyroxene crystals were separated by hand from rock crushes; the same visual inspection criteria were used as in the selection of feldspars. In general, NRM intensities of clinopyroxene were 1–3 times stronger than those of feldspars so an intensity cut-off was unnecessary. All the experiments were done within the magnetically shielded laboratory at the University of Rochester (<200 nT ambient field). Samples selected for study were heated inside a set of Mu-metal shields using a Synrad CO$_2$ laser for 90 seconds and then allowed to cool for 90 seconds, following the procedure described in Tarduno et al.[19]. All the samples were measured using a 2G DC SQUID magnetometer with high-resolution sensing coils at the University of Rochester. For the TTRM experiments, samples were stepwise thermally demagnetized above 520 °C (ref. [14]) (462 °C for the clinopyroxene sample) in a zero-field space. After the removal of NRM, the sample was heated a second time in a 60 µT field (30 µT for the clinopyroxene) applied along the laboratory z axis. The resulting TRM and NRM intensities were compared, using the following relationship, to estimate the palaeofield strength:

$$H_{palaeo} = \frac{NRM}{TRM} H_{lab} \qquad (2)$$

where H_{palaeo} and H_{lab} are the palaeo- and laboratory applied fields.

Thellier–Coe-style experiments. Samples were heated (following the above protocol) in ~100 °C steps to 320 °C, after which smaller (~10 to 25 °C) temperature steps were used until at least 95% of the NRM magnetization was removed. Thellier–Coe-style[34] PTRM steps were incorporated; PTRM checks were not begun until 360 °C for feldspars (340 °C for clinopyroxene) to limit the potential alteration during laboratory heating. Due to the weak NRM magnetizations of the feldspar samples, multiple measurements were collected and averaged for each step, and anomalous measurements (for example, flux jumps) were discarded. During field-on steps, a 15, 30 or 60 µT field was applied along the laboratory z axis during heating and cooling of the sample. Palaeointensity statistics[35,36] and the categorization of samples based on passage of reliability criteria are tabulated in Supplementary Table 2.

Anisotropy of thermal remanence. The anisotropy of thermal remanence experimental procedure was based on the protocol described by Veitch et al.[37].

During the course of a palaeointensity experiment, after the NRM begins to unblock, the anisotropy experiment is started. After the field-off step, the sample was heated to the same temperature in a 30 µT magnetic field for feldspar (15 µT for clinopyroxene) along the laboratory +z axis, after which the magnetization was measured. Field-on heating steps were repeated five additional times, with the field applied along orthogonal laboratory directions (+x, −x, +y, −y and −z). A multidomain tail check[38] was performed after the six total field-on steps to test for alteration; an experiment was accepted if the multidomain tail check was less than 10% of the PTRM value. For clinopyroxene, a PTRM check was used to assess the alteration (with a 10% agreement as the threshold for acceptance). Once completed, the palaeointensity experiment proceeded until the NRM was removed. Determination of the anisotropy correction factor from the orthogonally applied PTRMs during the anisotropy experiment allows a TRM susceptibility tensor to be constructed, and using the following equation an anisotropy correction factor is determined:

$$f_{aniso} = \frac{\kappa^{TRM} \mathbf{k}}{\kappa^{TRM} \mathbf{h}} \qquad (3)$$

where κ^{TRM} is the TRM susceptibility tensor, $\mathbf{k}$ is the unit vector of the applied field during laboratory heating and $\mathbf{h}$ is the unit vector of the NRM of the sample.

Data availability

Data presented here are available in the Earthref (MagIC) database (earthref.org/MagIC/16534).

References

34. Coe, R. S. The determination of paleo-intensities of the Earth's magnetic field with emphasis on mechanisms which could cause non-ideal behavior in Thellier's method. *J. Geomag. Geoelectr.* **19**, 157–179 (1967).
35. Shaar, R., Tauxe, L. & Thellier, G. U. I. An integrated tool for analyzing paleointensity data from Thellier-type experiments. *Geochem. Geophys. Geosys.* **14**, 677–692 (2013).
36. Coe, R. S., Grommé, S. & Mankinen, E. A. Geomagnetic paleointensities from radiocarbon-dated lava flows on Hawaii and the question of the Pacific nondipole low. *J. Geophys. Res.* **83**, 1740–1756 (1978).
37. Veitch, R. J., Hedley, I. G. & Wagner, J.-J. An investigation of the intensity of the geomagnetic field during Roman times using magnetically anisotropic bricks and tiles. *Arch. Sci.* **37**, 359–373 (1984).
38. Riisager, P. & Riisager, J. Detecting multidomain magnetic grains in Thellier palaeointensity experiments. *Phys. Earth Planet. Inter.* **125**, 111–117 (2001).